

Transcriptomic Signatures of Alterations in a Myoblast Cell Line Infected with Four Distinct Strains of *Trypanosoma cruzi*

Daniel Adesse,* Dumitru A. Iacobas, Sanda Iacobas, Luciana R. Garzoni, Maria de Nazareth Meirelles, Herbert B. Tanowitz, and David C. Spray

Laboratorio de Ultra-estrutura Celular, Instituto Oswaldo Cruz–Fiocruz, Rio de Janeiro, Brazil;
Dominick P. Purpura Department of Neuroscience, Albert Einstein College of Medicine, Bronx, New York;
Department of Pathology, Albert Einstein College of Medicine, Bronx, New York

Abstract. We examined the extent to which different *Trypanosoma cruzi* strains induce transcriptomic changes in cultured L₆E₉ myoblasts 72 hours after infection with Brazil (TC I), Y (TC II), CL (TC II), and Tulahuen (TC II) strains. Expression of 6,289 distinct, fully annotated unigenes was quantified with 27,000 rat oligonucleotide arrays in each of the four replicas of all control and infected RNA samples. Considering changes greater than 1.5-fold and *P* values < 0.05, the Tulahuen strain was the most disruptive to host transcriptome (17% significantly altered genes), whereas the Y strain altered only 6% of the genes. The significantly altered genes in the infected cells were largely different among the strains, and only 21 genes were similarly changed by all four strains. However, myoblasts infected with different strains showed proportional overall gene-expression alterations. These results indicate that infection with different parasite strains modulates similar but not identical pathways in the host cells.

INTRODUCTION

Chagas disease, caused by infection with the flagellate protozoan parasite *Trypanosoma cruzi*, is a widespread disease in Latin America affecting millions of people.¹ Infective trypomastigotes invade peripheral cells and transform into multiplicative amastigote forms. The initial (acute) phase of the disease is characterized by intense tissue parasitism involving the heart, skeletal and smooth muscle cells, liver, fat, and brain that is accompanied by intense focal inflammation and necrosis.² Some patients can evolve to a chronic phase of the disease that can include cardiac and/or digestive forms. The severity of the chronic phase may be related to the efficiency of the host immune response in resolving the infection during the acute phase,³ but this has never been proven. Moreover, there are several reports of differences of tropism of *T. cruzi* to host tissue, which is also associated with the pathogenesis of chronic Chagas disease.^{4,5}

Differences in the pathogenesis of the disease among patients may vary according to differences in both hosts and parasite strain.⁶ Among differences in *T. cruzi* strains are their resistance to chemotherapy, oxidative stress, and infectivity in the mouse.^{7–9} Although previous *in vivo* and *in vitro* microarray analyses using cultured cells^{10,11} and hearts of mice^{12–14} infected with *T. cruzi* showed that this infection results in profound alterations in the host cells, the degree to which these results are applicable to all *T. cruzi* strains found in infected individuals has not been explored previously.

Since host immune response, tissue parasitism, and parasite strains may be important factors in the pathogenesis of chronic Chagas disease, we have used gene-array analysis to compare the alterations in host cells caused by four different stocks of *T. cruzi*. The present study characterizes the transcriptomic changes in cultured rat myoblasts that result from infection with each strain and highlights common genes that were similarly or differentially modulated by each strain. Analysis reveals host cell changes that might lead to an understanding of previously observed differences in pathogenesis *in vivo*.

METHODS

Cells and parasites. The L₆E₉ rat myoblast cell line was maintained in Dulbecco's modified eagle medium (DMEM) supplemented with 10% fetal bovine serum (Invitrogen, Carlsbad, CA) and 1% penicillin/streptomycin at 37°C with 5% CO₂ atmosphere.¹⁵ Cells were dissociated with trypsin/ethylenediaminetetraacetic acid (EDTA) solution (Gibco), and 10⁶ cells were plated in 100-mm² cell-culture dishes. After 24 hours of plating, cells were washed with Phosphate Buffered Saline (PBS) containing Ca²⁺ and Mg²⁺ (Gibco) and infected with 2 × 10⁶ trypomastigote forms of *T. cruzi* in DMEM. Parasites of the Y, CL Brener,¹⁶ Tulahuen, and Brazil strains were obtained from supernatants of infected L₆E₉ cultures. Forty-eight hours post-infection, cells were washed twice with Ca²⁺/Mg²⁺ PBS to remove free trypomastigotes in the supernatant, and they were re-fed with fresh supplemented DMEM. Total RNA was harvested at 72 hours post-infection using guanidinium thiocyanate-phenol-chloroform extraction (TRIZOL) reagent (Invitrogen, Carlsbad, CA), following the protocol indicated by the manufacturer, when at least 25% of the cultured cells were infected, presented only intracellular amastigotes, and had no release of trypomastigotes, which would lead to re-infection of culture.

***T. cruzi* genotyping.** The different isolates of *T. cruzi* used in this work were identified using the method described by Fernandes and others¹⁷ according to their phylogenetic lineage. Briefly, genomic DNA from 5 × 10⁸ epimastigote forms of the Y, CL, Brazil, and Tulahuen strains was extracted using the DNeasy kit (Qiagen, Hilden, Germany). Multiplex polymerase chain reaction (PCR) was performed using 150 ng of DNA, and the primers were designed to recognize the mini-exon gene of the parasites using a pool of five nucleotides: three were derived from a hypervariable region of the *T. cruzi* mini-exon repeat (*T. cruzi* 1 [TC1], 5' ACA CTT TCT GTG GCG CTG ATC G; TC 2, 5' TTG CTC GCA CACTCG GCT GCA T; TC 3, 5' CCG CGW ACA ACC CCT MAT AAA AAT G) and an oligonucleotide from a specific region of the *Trypanosoma rangellii* non-transcribed spacer (TR; 5' CCT ATT GTG ATC CCC ATC TTC G). A common downstream oligonucleotide corresponds to sequences present in the most conserved region of the mini-exon gene (ME;

*Address correspondence to Daniel Adesse, Avenida Brasil 4365, Pavilhão Carlos Chagas, Rio de Janeiro, Rio de Janeiro, Brazil. E-mail: adesse@ioc.fiocruz.br

5' TAC CAA TAT AGT ACA GAA ACT G). PCR reaction was performed using the Multiplex PCR kit (Qiagen) with the initial denaturing cycle of 95°C (15 seconds) followed by 30 cycles of 94°C (30 seconds, denaturing), 60°C (30 seconds, annealing), and 72°C (30 seconds, extension); a final extension cycle of 72°C lasts for 10 minutes and is followed by a soak cycle (4°C) using a PTC-100 Thermocycler (M.J. Research Inc., Massachusetts, USA). PCR fragments were loaded into a 2% agarose/ Tris base, boric acid, EDTA (TBE) gel with 0.008% ethidium bromide, and images were acquired using Kodak 1D Scientific Imaging Systems.

Light microscopy. Cells (6×10^4) were plated into glass cover slips in 24-well plates. After 24 hours, 10^6 trypomastigotes were added to cultures in fresh supplemented DMEM, and infection was followed as described above. After 72 hours of infection, cells were washed three times and fixed with glutaraldehyde for Giemsa staining.¹⁸ Cover slips were digitally photographed using a Zeiss Axioplan microscope.

Microarray analysis. We used the protocol optimized in our laboratory¹⁹ according to the standards of the Microarray Gene Expression Data Society. Briefly, 20 μ g Trizol extracted total RNA from each culture dish was reverse transcribed in the presence of fluorescent Alexa Fluor 555-aha-dUTP (green fluorescent emission) or Alexa 647-aha-dUTP (red emission; Invitrogen) to label cDNAs. Differently labeled RNA samples from biological replicas of control (uninfected cells cultured for the same duration) or infected with one strain at a time were co-hybridized ("multiple yellow" strategy²⁰) overnight at 50°C

with rat 27k oligonucleotide arrays printed by Duke University (full technical information available at <http://www.ncbi.nlm.nih.gov/geo/query/acc.cgi?acc=GSE18175>). All spots affected by local corruption, with saturated pixels, or with foreground fluorescence less than twice the background fluorescence (where noise may obscure the quantity) were removed from the analysis. The background subtracted signals were normalized iteratively,¹⁹ alternating red/green, interblock, lowess and scale intraslide and interslide normalization until the fluctuation of the ratio between the spot median and the corresponding block median of valid spots became less than 5% between successive iteration steps. Normalized expression levels were organized into redundancy groups (each group composed of all spots probing the same gene) and were represented by the weighted average of the values of individual spots. The abundance of host cell transcripts was considered as significantly altered after infection if the absolute fold-change was greater than 1.5-fold and the *P* value of the heteroscedastic *t* test (two-sample, unequal variance), applied to the means of the background-subtracted normalized fluorescence values in the four biological replicas of the compared transcriptomes, was greater than 0.05. This composite criterion to identify the significantly altered gene expression minimizes the number of false hits without eliminating too many true hits. The 50% change cut-off (1.5-fold) was selected to be significantly larger than the overall less than 10% interslide technical noise determined for the bacterial controls.

Gene categories. GenMapp and MappFinder programs (www.genmapp.org; Gladstone Institute, University of California,

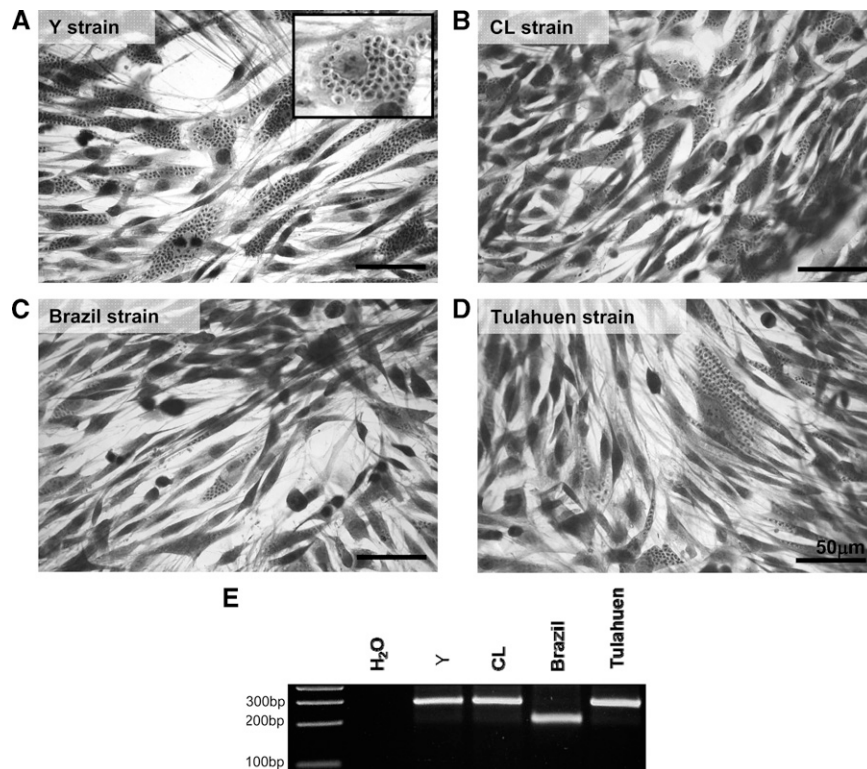


FIGURE 1. Characterization of L_6E_0 cell infection by four *T. cruzi* strains. Giemsa staining of L_6E_0 cells after 72 hours of infection with (A) Y, (B) CL, (C) Brazil, and (D) Tulahuen strains of *T. cruzi* was performed. All strains studied successfully infected the myoblasts, and at 72 hours post infection (hpi), it was possible to observe amastigote forms in the host cell's cytoplasm as shown in details in A inset. (Bars = 50 μ m.) To confirm genetic background of the parasite stocks used for infection, genomic DNA from epimastigote forms was isolated and amplified with Multiplex PCR with primers derived from a hypervariable region of the *T. cruzi* mini exon. (E) The Y, CL, and Tulahuen strains had a PCR product of 250 bp, indicating that they belong to the *T. cruzi* (TC) II family, and the Brazil strain had a 200-bp product, indicating that it belongs to TC I family.

San Francisco, CA) were used to determine whether or not altered gene expressions differed significantly from chance for the overlapping functional and structural Gene Ontology (GO) categories.

RESULTS

Multiplex PCR was performed to confirm correspondence of the strains of *T. cruzi* used in this work to the phylogenetic classification as described in the literature. We verified that the Y, CL, and Tulahuen parasites displayed a 250-bp PCR product, indicating that they belong to the *T. cruzi* II (TC II) group. The Brazil strain, whose effects in host cells and animals have been characterized previously by our group,^{15,21} belongs to the TC I group, because it displays a 200-bp PCR product (Figure 1E).

Data complying with the Minimum Information about Microarray Experiments (MIAME) were deposited in the National Center for Biotechnology Information (NCBI) database (<http://www.ncbi.nlm.nih.gov/geo/query/acc.cgi?acc=GSE18175>) as series GSE18175. In this experiment, we quantified 6,289 distinct, well-annotated unigenes in all samples.

The impact of infection with each of the four strains of *T. cruzi* on the transcriptome changes of the same immortalized cell line was strikingly different (Figure 2). Thus, as shown in Table 5, there were only two (0.03%) genes significantly decreased, and 19 (0.3%) increased by all four *T. cruzi* strains. However, 4,340 (69%) genes were not significantly altered by any of the strains. The Venn diagrams in Figure 2 illustrate this observation by showing the number of genes equally increased (Figure 2B) or decreased (Figure 2C) by two, three, or all four strains of *T. cruzi*.

Analysis of functional classes of genes modulated by the infection with different *T. cruzi* strains was performed with GenMapp software, and it revealed a very small number of gene functional categories with an abundance that was similarly affected by each pair of parasite strains (Table 7). Below, we describe in more detail the differences that were observed.

Y strain. We observed that the Y strain altered expression of 426 (6%) of the 6,996 quantified host cell genes. Among these genes, 150 were decreased, and 276 were increased after 72 hours of infection. When we identified individual genes whose expression was altered exclusively by the Y strain, we found that 87 genes were increased, such as α -1-integrin (1.76-fold), intercellular adhesion molecule (1.79-fold), presenilin 2 (3.81-fold), transforming growth-factor beta regulated gene (1.73-fold), and vascular cell-adhesion molecule 1 (1.91-fold). Sixty-five genes were decreased, such as cardiac Ca^{2+} ATPase (-1.6-fold), cadherin (-2.88-fold), and Cyp26b1 (cytochrome P450, family 26, subfamily b, polypeptide 1; -2.83-fold) (Table 1). The Y strain affected the expression of 11 gene categories including calcium and metal binding, regulation of transcription, and complexes of protein (Table 7).

CL strain. When the rat myoblasts were infected with the CL strain, we observed that 763 of 7,133 (11%) genes were significantly altered (53 decreased and 710 increased). The CL strain uniquely modulated the expression of 517 genes (494 were increased and 23 decreased), which corresponded to alterations in 14 gene categories including protein, intracellular protein, proton and ion transport, and ubiquitin cycle (Table 7). Some of the genes that the CL strain modulated were adenylate

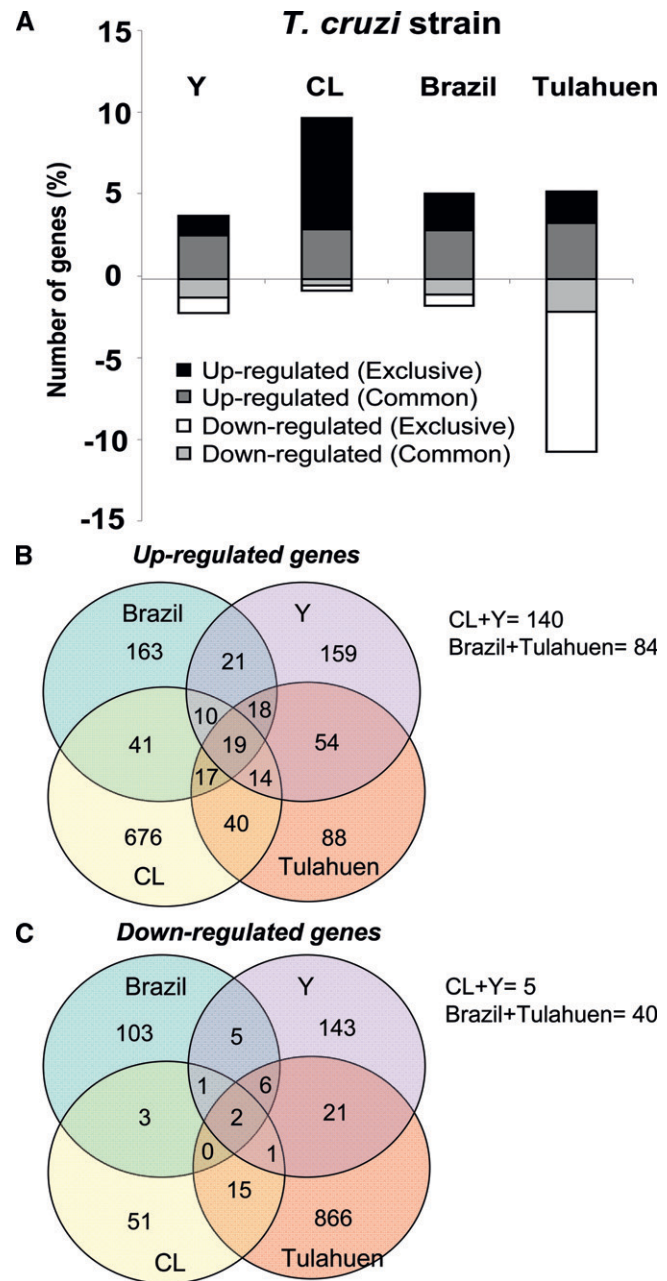


FIGURE 2. Profiles of transcriptomic changes caused by each strain of *T. cruzi* in host cells. The percentage of genes modulated in L_6E_9 cells by each *T. cruzi* strain is shown in A. Genes with fold-change value ≥ 1.5 and P value ≤ 0.05 were quantified and plotted in this histogram, in which bars represent a percentage of the valid genes. Bars in white and black represent genes whose expression was decreased or increased exclusively by each strain, respectively. Bars in gray and light gray represent genes that were increased and decreased, respectively, and shared this modulation by at least two strains. The Venn diagrams represent the number of genes significantly (fold change ≥ 1.5 and P value < 0.05) (B) increased and (C) decreased in common by all four strains, by three strains, by pairs of strains, and by individual strains of the parasite. The number of genes equally altered by CL + Y and Brazil + Tulahuen strains is indicated below the diagrams. Note the low number of genes altered in the same direction by all strains studied (19 increased and 2 decreased).

cyclase 2 (1.56-fold), α -spectrin (1.7-fold), annexin A1 (1.7-fold), caspase 7 (1.76-fold), epsin 2 (1.97), glutamate receptor (3.38), matrix metalloproteinase (MMP) 3 (2.51-fold), and syntaxin (-1.56-fold) (Table 2).

TABLE 1
Y Strain

Gene name	Gene symbol	Fold change
Alanyl-tRNA synthetase	Aars	1.85
Actin, gamma, cytoplasmic 1	Actg1	1.55
Chloride intracellular channel 2	Clic2	1.55
Cyclin-dependent kinase inhibitor 2B (p15; inhibits CDK4)	Cdkn2b	1.65
Glycogen synthase kinase 3 beta	Gsk3b	1.52
Integrin alpha 1	Itga1	1.76
Intercellular adhesion molecule 1	Icam1	1.79
Lectin, galactose binding, soluble 3	Lgals3	1.52
Presenilin 2	Psen2	3.814
Protein C receptor, endothelial	Procr	2.04
Pyruvate kinase, muscle	Pkm2	1.70
Syndecan -protein	Sdcbp	1.854
Transforming growth-factor beta-regulated gene 1	Tbrg1	1.73
Vascular cell-adhesion molecule 1	Vcam1	1.91
X-linked myotubular myopathy gene 1	Mtm1	1.53
Actin, alpha 1, skeletal muscle	Acta1	-4.84
Acyl-CoA synthetase long-chain family member 3	Acsl3	-2.63
ATPase, Ca++ transporting, cardiac muscle, slow twitch 2	Atp2a2	-1.60
Cadherin 15	Cdh15	-2.88
Calsenilin, presenilin-binding protein, EF hand transcription factor	Csen	-1.62
Cytochrome P450, family 26, subfamily b, polypeptide 1	Cyp26b1	-2.83
Guanine monophosphate synthetase	Gmps	-1.94
Myosin light chain, phosphorylatable, fast skeletal muscle	Mylpf	-1.68
Rho family GTPase 2	Rnd2	-1.62

Brazil strain. The Brazil strain induced significant alteration of 7.31% genes of *L₆E₉* by more than 1.5-fold. Among these 494 modulated genes, 117 were decreased, and 377 were increased. Some interesting genes that had their transcription altered by infection with the Brazil strain were cardiomyopathy

TABLE 2
CL strain

Gene name	Gene symbol	Fold change
Adenylate cyclase 2	Adcy3	1.56
Alpha-spectrin 2	Spna2	1.70
Angiopoietin-like 2	AF159049	1.56
Annexin A1	Anxa1	1.56
Casein kinase 1, gamma 1	Csnk1g1	1.95
Caspase 7	Casp7	1.76
Chemokine-like factor	Cklf	1.76
Chondroitin sulfate proteoglycan 6	Cspg6	1.64
Desmuslin	Dmn	1.60
Epsin 2	Epn2	1.97
Glutamate receptor, ionotropic, N-methyl D-aspartate 2B	Grin2b	3.38
Integrin alpha 5	Itga5	1.84
Interleukin 1 receptor, type I	Il1r1	2.27
Matrix metalloproteinase 10	Mmp10	2.40
Matrix metalloproteinase 3	Mmp3	2.52
Phosphatidylethanolamine N-methyltransferase	Pemt	2.03
Phospholipase D1	Pld1	1.58
Plasminogen activator, urokinase receptor	Plaur	1.76
Proteasome (prosome, macropain) 26S subunit, non-ATPase, 2	Psm2	1.99
Chaperonin subunit 4 (delta)	Cct4	-1.57
Syntaxin 8	Stx8	-1.56
T-cell immunomodulatory protein	Cda08	-2.61

TABLE 3
Brazil strain

Gene name	Gene symbol	Fold change
H2A histone family, member Y	H2afy	3.70
Cardiomyopathy associated 3	Cmya3	3.37
Protein kinase C, gamma	Prkcc	2.70
Myocyte enhancer factor 2D	Mef2d	2.43
Mitogen-activated protein kinase 9	Mapk9	2.12
Fibroblast growth factor 21	Fgf21	1.95
ATPase, H+/K+ exchanging, beta polypeptide	Atp4b	1.90
Phosphatidylinositol 3-kinase, C2 domain containing, gamma polypeptide	Pik3c2g	1.78
Paladin	Pald	1.67
Desmin	Des	1.63
Phosphatidylinositol 3 kinase, regulatory subunit, polypeptide 3	Pik3r3	-1.53
Coronin, actin-binding protein, 1B	Coro1b	-1.91
Synaptotagmin XI	Syt11	-1.91
Proteasome (prosome, macropain) 28 subunit, beta	Psme2	-2.35
Keratin 25D	Krt25d	-2.38
Tropomyosin 4	Tpm4	-2.46

associated gene (3.37-fold), MMP 1B (2.44-fold), mitogen-activated protein kinase 9 (2.12-fold), fibroblast growth factor (1.94-fold), desmin (1.63-fold), and tropomyosin 4 (-2.45-fold) (Table 3). Ten functional categories of genes were highly modulated in *L₆E₉* by Brazil strain, including metalloproteinase

TABLE 4
Tulahuen strain

Gene name	Gene symbol	Fold change
Activin A receptor type II-like 1	Acvr1l	7.60
Cadherin 3, type 1, P-cadherin (placental)	Cdh3	4.65
Cardiac ankyrin repeat kinase	Cark	2.54
CDK5 regulatory subunit-associated protein 1	Cdk5rap1	2.40
Chymotrypsinogen B	Ctrb	2.64
Glucose 6 phosphatase, catalytic, 3	G6pc3	1.65
Inositol 1,4,5-trisphosphate 3-kinase C	Itpkc	2.37
Interleukin 11	Il11	1.68
Kinesin family member C1	Kifc1	2.04
Myotrophin	Mtpn	1.51
ATPase, Ca++ transporting, plasma membrane 1	Atp2b1	-2.76
Bcl2 modifying factor	Bmf	-2.93
Calcium channel, voltage-dependent, beta 3 subunit	Cacnb3	-1.88
Calreticulin	Calr	-2.04
Caspase 9	Casp9	-1.75
Cytochrome c oxidase, subunit Va	Cox5a	-1.62
Cytokine-induced apoptosis inhibitor 1	Ciapin1	-1.67
Dynein cytoplasmic 1 heavy chain 1	Dync1h1	-1.86
Ectonucleoside triphosphate diphosphohydrolase 1	Entpd1	-2.90
Farnesyltransferase, CAAX box, alpha	Fnta	-1.66
Hypoxia inducible factor 1, alpha subunit	Hif1a	-1.52
Inositol 1,4,5-triphosphate receptor 3	Itp3	-3.70
Janus kinase 3	Jak3	-1.64
Junctional adhesion molecule 3	Jam3	-2.25
Laminin, beta 2	Lamb2	-2.21
Matrix metalloproteinase 11	Mmp11	-3.46
Muscle, skeletal, receptor tyrosine kinase	Musk	-2.73
Phospholipase D2	Pld2	-2.88
Protein kinase C, nu	Prkc	-2.57
Synaptojanin 2	Synj2	-2.35
Troponin T2, cardiac	Tnnt2	-2.89
Tumor protein p53	Tp53	-1.92

TABLE 5
Similar results

Gene name	Gene symbol	Fold change (strains)			
		Brazil	CL	Tulahuen	Y
C1q and tumor necrosis factor-related protein 1	C1qTNF1	-1.90	-1.80	-2.70	-1.80
Matrix metalloproteinase 14	MMP14	-2.00	-1.90	-2.00	-1.70
Cardiotrophin-like cytokine factor 1	Clcf1	2.20	2.30	1.80	2.30
Cut-like 1 (<i>Drosophila</i>)	Cutl1	7.72	2.58	5.36	1.59
DNA-damage inducible transcript 3	Ddit3	9.30	3.08	2.41	2.64
Excision repair cross-complementing rodent repair deficiency, complementation group 3	Ercc3	2.19	2.67	1.59	2.36
G protein-coupled receptor, family C, group 5, member A	Gprc5a	1.94	2.53	1.87	1.99
GrpE-like 1, mitochondrial	Grpel1	1.60	1.95	1.66	1.91
Pericentriolar material 1	Pcm1	2.70	4.25	2.23	3.70
Proprotein convertase subtilisin/kexin type 7	Pcsk7	6.93	2.87	2.38	2.15
Serologically defined colon cancer antigen 3	Sdccag3	3.36	2.71	2.67	2.50
Solute carrier family 1 (glutamate/neutral amino acid transporter)	Slc1a4	1.59	2.50	1.82	1.68
Tyrosine 3-monooxygenase/tryptophan 5-monooxygenase activation protein	Ywhaq	2.84	2.85	1.77	2.56

activity, small GTPase-mediated signal transduction, and ubiquitin cycle (Table 7).

Tulahuen strain. The Tulahuen strain of *T. cruzi* induced the highest percentage of altered gene expression in the myoblasts (17.35%) with 761 decreased genes and 383 increased genes, of which, 617 and 139, respectively, were uniquely observed in Tulahuen-infected dishes. Additionally, infection with this strain significantly modulated the expression of 18 gene categories, including cholesterol biosynthesis, immune response, lipid metabolism, and receptor activity (Table 7). Some relevant examples of host cell genes significantly modulated during infection were p-cadherin (4.64-fold), cardiac ankyrin repeat kinase (2.54-fold), chymotrypsinogen B (2.64-fold), H2A histone family member Z (3.18-fold), interleukin 11 (1.68-fold), myotrophin (1.51-fold), caspase 9 (-1.75-fold), cytochrome c oxidase, subunit Va (-1.61-fold), heavy and light chain dynein (-1.86- and -1.81-fold, respectively), farnesyltransferase (-1.65-fold), hypoxia-inducible factor 1 α subunit (-1.51-fold), janus kinase 3 (-1.64-fold), matrix metalloproteinase 11 (-3.46-fold), and cardiac troponin T2 (-2.89-fold) (Table 4).

Genes modulated equally by all *T. cruzi* strains as possible disease biomarkers. We observed that 13 (0.18%) host cell genes had the same pattern of significant modulation by all four strains of *T. cruzi* studied. These genes, thus, may represent

disease biomarkers that could be useful in detecting the disease independent of the parasite strain. Only two (0.027%) were decreased, MMP-14 (-1.9-fold) and C1q and tumor necrosis factor-related protein 1 (-2.0-fold), and 11 (0.15%) increased, such as solute carrier family 1 (glutamate/neutral amino acid transporter; 1.9-fold), G protein-coupled receptor (2.1-fold), cardiotrophin-like cytokine factor 1 (2.13-fold), pericentriolar material 1 (3.22-fold), and DNA damage-inducible transcript 3 (4.37-fold). Table 5 shows the list of these thirteen genes and their modulation by each strain of the parasite. GenMapp analysis revealed that only nine gene categories were equally expressed by some pairs of strains such as receptor activity (Brazil and Tulahuen) and ubiquitin cycle (Brazil and CL) (Table 7).

Oppositely modulated genes. Surprisingly, our arrays revealed that some transcripts increased by one specific strain were decreased by another strain. Table 6 contains all the 24 genes that behaved in this manner. Some genes of interest were cytochrome P450, family 2, subfamily d, polypeptide 22 (3-fold by Brazil strain and -2.9-fold by Y strain), neuropathy target esterase-like 1 (2.1-fold by Y strain and -1.8-fold by CL strain), platelet-derived growth-factor receptor, β polypeptide (1.7-fold by CL strain and -1.6-fold by Tulahuen strain), protein kinase D2 (1.5-fold by Brazil strain and -1.6-fold by Y strain), and RNA polymerase 1-1 (1.6-fold by CL strain and -1.6-fold by Tulahuen strain).

TABLE 6
Opposite results

Gene name	Gene symbol	Fold change (strains)			
		Brazil	CL	Tulahuen	Y
ADP-ribosylation factor guanine nucleotide-exchange factor 2	Arfgef2	-	1.56	-1.54	-
CDC-like kinase 2	LOC365842	-	1.52	-1.64	-
Cytochrome P450, family 2, subfamily d, polypeptide 22	Cyp2d22	2.97	-	-	-2.92
NAD synthetase 1	Nadsyn1	-	1.56	-1.63	-
Neuropathy target esterase-like 1	Ntel1	-	-1.78	-	2.11
Platelet-derived growth-factor receptor, beta polypeptide	Pdgfrb	-	1.68	-1.64	-
Pleckstrin homology, Sec7, and coiled-coil domains 1	Pscd1	-	1.53	-1.53	-
Preoptic regulatory factor-2	PORF-2	-	1.62	-1.56	-
Protein kinase D2	Prkd2	1.50	-	-	-1.62
Regenerating islet-derived 1	Reg1	1.67	-2.31	-	-
RNA polymerase 1-1	Rpo1-1	-	1.56	-1.56	-
Son of sevenless homolog 1	Sos1	-1.53	1.82	-	-
Sulfotransferase family 1A, phenol-preferring, member 1	Sult1a1	-	-	1.90	-1.53
Thymoma viral proto-oncogene 2	Akt2	-	1.54	-1.64	-
Transducer of ErbB-2.1	Tob1	-	-	1.58	-1.72

TABLE 7
Gene categories

Gene Ontology (GO) ID	GO Name	No. changed	No. measured	No. in GO	Percent changed	P value
Y strain						
5634	Nucleus	22	557	1,643	3.95000	0.004
45449	Regulation of transcription	12	264	884	4.55000	0.010
6355	Regulation of transcription, DNA-dependent	11	237	790	4.64000	0.012
5509	Calcium-ion binding	8	149	538	5.37000	0.013
6350	Transcription	12	278	920	4.32000	0.014
46872	Metal-ion binding	20	593	1,913	3.37000	0.049
5743	Mitochondrial inner membrane	4	22	63	18.18000	0.006
19866	Organelle inner membrane	4	29	79	13.79000	0.026
16757	Transferase activity, transferring glycosyl groups	5	48	144	10.42000	0.042
43234	Protein complex	9	396	1,280	2.27000	0.052
16853	Isomerase activity	4	34	74	11.77000	0.052
CL strain						
5829	Cytosol	4	68	121	5.88000	0.002
5622	Intracellular	18	1,331	3,766	1.35000	0.004
15031	Protein transport	5	154	348	3.25000	0.011
6512	Ubiquitin cycle	3	102	281	2.94000	0.049
3824	Catalytic activity	8	1,611	5,073	0.50000	0.054
6886	Intracellular protein transport	3	103	237	2.91000	0.054
16757	Transferase activity, transferring glycosyl groups	10	48	144	20.83000	0.011
15992	Proton transport	6	24	64	25.00000	0.023
4197	Cysteine-type endopeptidase activity	7	34	91	20.59000	0.032
6811	Ion transport	18	118	555	15.25000	0.038
3924	Gtpase activity	5	22	45	22.73000	0.040
16491	Oxidoreductase activity	25	185	539	13.51000	0.045
6812	Cation transport	14	86	375	16.28000	0.046
Brazil strain						
8237	Metallopeptidase activity	3	38	133	7.89000	0.020
4984	Olfactory receptor activity	9	24	1,034	37.50000	0.000
1584	Rhodopsin-like receptor activity	9	46	1,391	19.57000	0.001
4872	Receptor activity	20	195	2,013	10.26000	0.002
7186	G-protein-coupled receptor protein-signaling pathway	11	82	1,581	13.41000	0.005
43234	Protein complex	12	396	1,280	3.03000	0.022
7264	Small gtpase mediated signal transduction	8	66	179	12.12000	0.027
5615	Extracellular space	4	23	136	17.39000	0.029
6512	Ubiquitin cycle	1	102	281	0.98000	0.046
5525	GTP binding	10	99	237	10.10000	0.050
Tulahuen strain						
6457	Protein folding	16	68	138	23.53000	0.001
5488	Binding	219	1,786	5,708	12.26000	0.010
3743	Translation initiation factor activity	7	25	37	28.00000	0.019
6695	Cholesterol biosynthesis	4	11	15	36.36000	0.021
6955	Immune response	10	46	258	21.73913	0.033
6629	Lipid metabolism	20	120	304	16.67000	0.053
4984	Olfactory receptor activity	7	24	1,034	29.17000	0.000
1584	Rhodopsin-like receptor activity	9	46	1,391	19.57000	0.001
16020	Membrane	63	740	3,798	8.51000	0.003
19866	Organelle inner membrane	7	29	79	24.14000	0.003
5743	Mitochondrial inner membrane	5	22	63	22.73000	0.012
4872	Receptor activity	20	195	2,013	10.26000	0.014
16021	Integral to membrane	41	494	2,888	8.30000	0.018
5856	Cytoskeleton	13	114	337	11.40000	0.021
7186	G-protein-coupled receptor protein-signaling pathway	10	82	1,581	12.20000	0.029
9058	Biosynthesis	9	284	923	3.17000	0.036
16874	Ligase activity	2	124	329	1.61000	0.046
5739	Mitochondrion	15	149	290	10.07000	0.048

Correlations between infections with four strains. Our studies identifying individual genes that were significantly altered by the four strains of *T. cruzi* revealed a surprising diversity with only a few genes similarly changed by infection with all strains. However, because this analysis selects only individuals, it does not compare subtle global changes throughout the transcriptome. To compare global transcriptomic alteration

patterns in L₆E₉ cells infected by the four strains used in the current investigation, we compared the entire gene-array datasets obtained from the infection with each strain against each of the other strains. With Origin software (OriginLab, Northampton, MA), we plotted results of these pairs as log₂ values of their expression ratios. In all six of the comparisons of expression changes induced by infection with separate

T. cruzi strains (Figure 3), the regression coefficients (r^2 values) for these linear relations were highly significant, and P values in all cases were less than 0.0001. This finding indicates that although infection with each of the parasite strains leads to only partially overlapping alterations in the genes that are most affected, there is an overall similarity in the pattern of gene-expression alterations resulting from infection with all the strains.

DISCUSSION

Chagas disease represents a spectrum of pathogenesis, varying both in its severity and the organ systems afflicted. Although various host factors, such as competence to launch immune response, may account in part for differences in the pathogenesis of the disease, parasite strain is also an important variable,⁶ resulting in differences in viability, infectivity, and

tissue tropism.⁷⁻⁹ The present study was undertaken to evaluate the extent to which global gene-expression alteration was similarly altered after *in vitro* infection of a myoblast cell line with four distinct *T. cruzi* strains.

The microarray analyses described in this study were performed on the myoblast cell line L₆E₀ during infection with four reference strains of *T. cruzi*, each with well-characterized rates of *in vivo* and *in vitro* infectivity, resistance to chemotherapy, and pathogenesis *in vivo*. We used the Y and CL strains as representatives of the TC II group of *T. cruzi*, known to be found in central and eastern Brazil, which is commonly associated with the “mega” syndromes (cardiomegaly, megacolon, and megaesophagus).²² The Tulahuen strain was chosen to represent the TC I group, however, the Multiplex PCR performed with genomic DNA of parasites of this strain revealed that it was actually a strain belonging to the TC II family. The Brazil strain was selected, because

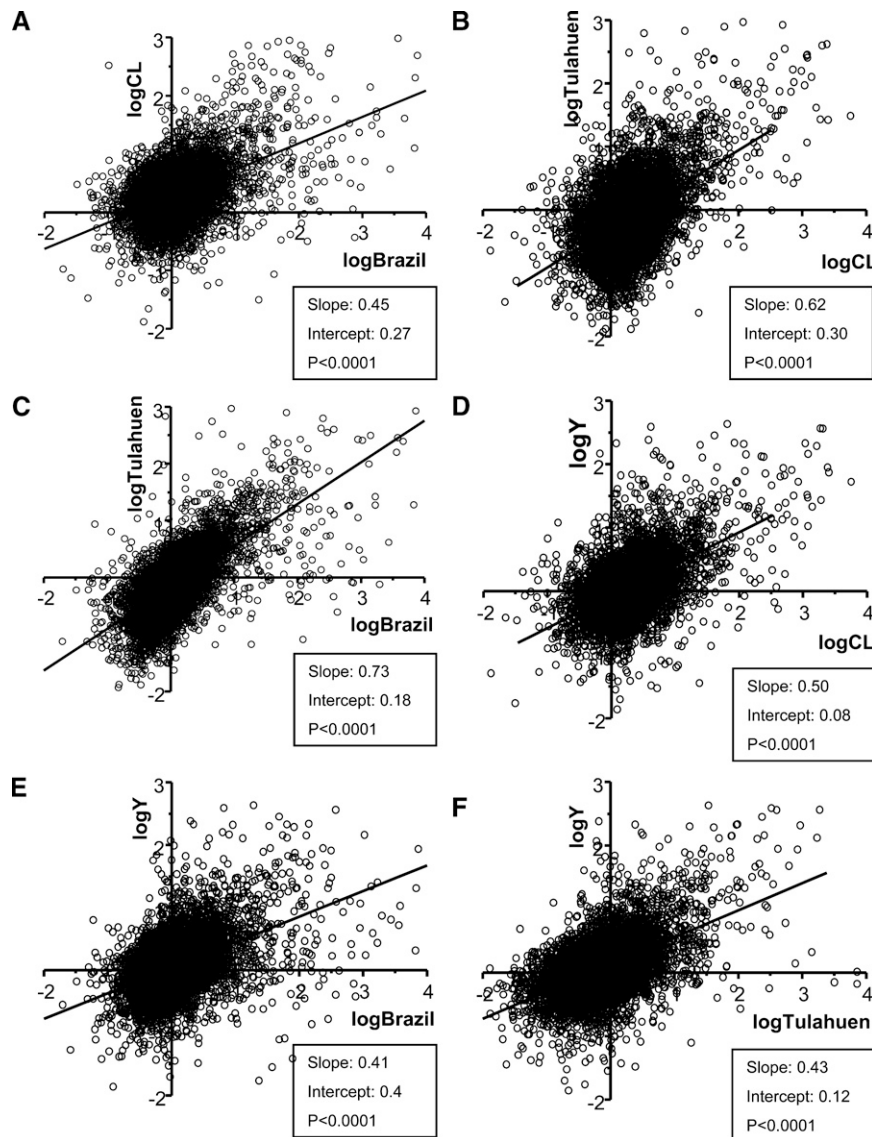


FIGURE 3. Correlation of datasets obtained by microarray analyses of the infection of L₆E₀ cell line with Y, CL, Brazil, and Tulahuen strains of *T. cruzi*. The datasets of each strain were plotted against each other in pairs of parasite strains. The histograms show how the transcriptomic changes induced by all strains have a highly significant correlation (all have P values < 0.0001). R^2 values were (A) 0.5, (B) 0.51, (C) 0.67, (D) 0.52, (E) 0.47, and (F) 0.53.

it has been shown to cause a dilated cardiomyopathy associated with a reduction in fractional shortening and myocardial wall thinning in mice.¹³ Genotyping revealed that the Brazil strain belongs to the TC I group, the predominant group in Venezuela and central Brazil, which is usually associated with electrocardiographic (ECG) abnormalities.²²

We have compared the datasets obtained from the microarray analyses in two ways, resulting in different but complementary conclusions regarding the pathogenesis of *T. cruzi* infection *in vitro* and perhaps, applicable to *in vivo* infection as well. First, through identification of the genes that had altered expression after infection, we identified a large number of gene expression changes in the infected cells, but only a very small number of these were common to infection with each parasite strain. We concluded from this analysis that each strain induces a particular fingerprint of pathology. One such fingerprint may include genes encoding cell-junction proteins, which was evidenced by our finding that both Tulahuen and Y strains down-regulated several cellular junction genes such as junction plakoglobin, junctional adhesion molecule 3, and adipocyte-specific adhesion molecule as well as cadherin 15 (Y strain). *T. cruzi* infection was also shown to alter adhesion molecules of the host such as connexin43²³ and cadherin-catenin.^{11,24} These findings highlight an evolving concept that many types of cardiomyopathy target expression or involve mutations in molecular components of the intercalated disk (see reference 25 for review and reference 26 for changes in sepsis). Thus, as pointed out in a recent review,²⁷ cardiomyopathies, including chronic chagasic cardiomyopathy, may be considered to be junctionopathies.

An additional conclusion from the small number of genes found to be commonly regulated in infections with all strains (e.g., cut-like 1, DNA-damage inducible transcript 3, proprotein convertase subtilisin/kexin type 7) may provide a subset of biomarkers that could be potentially useful for diagnosis of acute *T. cruzi* infection and possibly, also reliably determine both indeterminate phase and chronic disease.

The second type of analysis that we performed on the gene-expression datasets was to compare overall transcriptomic changes in myoblasts infected with each *T. cruzi* strain through regression analysis of relative expression levels of each gene. For this, we compared each of the six pair-wise combinations of parasite strains, in each case finding a highly significant positive slope. This analysis emphasizes the concept that although Chagas disease shows a spectrum of manifestations, it does indeed represent a syndrome of common phenotypic alterations. The shallow slopes of the regression lines indicate that the changes induced by the parasite strains, although similar, are on average very low in amplitude; this emphasizes again the potential utility of the few commonly altered biomarkers.

The significant alteration in few overlapping genes among myoblasts infected with all strains poses a formidable challenge to the development of disease biomarkers that can be used to detect disease endemic areas where endogenous infective strains differ, although the few genes that we have detected with strong and significant expression changes offer such a possibility. Nevertheless, the overall transcriptomic signature of the disease that is revealed in the strong correlations between subtle expression alteration of all genes may provide a source whereby additional biomarkers may be discovered as common principal components of the acute response.

Received July 17, 2009. Accepted for publication October 25, 2009.

Acknowledgments: The authors thank Vicki L. Braunstein (AECOM) and Angela Santos (LUC-Fiocruz) for the technical support with maintenance of the *T. cruzi* strains and Nadia Nehme and Dr. Octavio Fernandes (Fiocruz) and Aisha Cordero (AECOM) for the assistance with *T. cruzi* genotyping. We also thank Ethan Mackenzie (AECOM) for the help with GenMapp analysis. D.A. was supported in part by a grant from the Fogarty International Center-NIH D43 W007129 (HBT) and grants from The US National Institutes of Health AI-076248 (HBT), HL-73732 (HBT, DCS) and from CNPq, CNPq, PAPES IV-FIOCRUZ.

Authors' addresses: Daniel Adesse, Luciana Ribeiro Garzoni, and Maria de Nazareth Meirelles, Laboratório de Ultraestrutura Celular, Instituto Oswaldo Cruz, FIOCRUZ, Rio de Janeiro, Brazil. Dumitru A. Iacobas, Sanda Iacobas, and David C. Spray, Dominick P. Purpura Department of Neuroscience, Albert Einstein College of Medicine, Bronx, NY. Herbert B. Tanowitz, Department of Pathology, Albert Einstein College of Medicine, Bronx, NY.

REFERENCES

- de Souza W, 2007. Chagas' disease: facts and reality. *Microbes Infect* 9: 544-545.
- Tanowitz HB, Kirchhoff LV, Simon D, Morris SA, Weiss LM, Wittner M, 1992. Chagas' disease. *Clin Microbiol Rev* 5: 400-419.
- Higuchi Mde L, Benvenuti LA, Martins Reis M, Metzger M, 2003. Pathophysiology of the heart in Chagas' disease: current status and new developments. *Cardiovasc Res* 60: 96-107.
- Carneiro M, Romanha AJ, Chiari E, 1991. Biological characterization of *Trypanosoma cruzi* strains from different zymodemes and schizodemes. *Mem Inst Oswaldo Cruz* 86: 387-393.
- Andrade SG, 1999. *Trypanosoma cruzi*: clonal structure of parasite strains and the importance of principal clones. *Mem Inst Oswaldo Cruz* 94 (Suppl 1): 185-187.
- Andrade SG, Magalhães JB, 1996. Biodemes and zymodemes of *Trypanosoma cruzi* strains: correlations with clinical data and experimental pathology. *Rev Soc Bras Med Trop* 30: 27-35.
- Veloso VM, Carneiro CM, Toledo MJ, Lana M, Chiari E, Tafuri WL, Bahia MT, 2001. Variation in susceptibility to benznidazole in isolates derived from *Trypanosoma cruzi* parental strains. *Mem Inst Oswaldo Cruz* 96: 1005-1011.
- Mielniczki-Pereira AA, Chiavegatto CM, López JA, Colli W, Alves MJ, Gadelha FR, 2007. *Trypanosoma cruzi* strains, Tulahuen 2 and Y, besides the difference in resistance to oxidative stress, display differential glucose-6-phosphate and 6-phosphogluconate dehydrogenases activities. *Acta Trop* 101: 54-60.
- Sanchez G, Wallace A, Olivares M, Diaz N, Aguilera X, Apt W, Solari A, 1990. Biological characterization of *Trypanosoma cruzi* zymodemes: *in vitro* differentiation of epimastigotes and infectivity of culture metacyclic trypomastigotes to mice. *Exp Parasitol* 71: 125-133.
- Shigihara T, Hashimoto M, Shindo N, Aoki T, 2008. Transcriptome profile of *Trypanosoma cruzi*-infected cells: simultaneous up- and down-regulation of proliferation inhibitors and promoters. *Parasitol Res* 102: 715-722.
- Imai K, Mimori T, Kawai M, Koga H, 2005. Microarray analysis of host gene-expression during intracellular nests formation of *Trypanosoma cruzi* amastigotes. *Microbiol Immunol* 49: 623-631.
- Mukherjee S, Belbin TJ, Spray DC, Iacobas DA, Weiss LM, Kitsis RN, Wittner M, Jelicks LA, Scherer PE, Ding A, Tanowitz HB, 2003. Microarray analysis of changes in gene expression in a murine model of chronic chagasic cardiomyopathy. *Parasitol Res* 91: 187-196.
- Mukherjee S, Nagajyothi F, Mukhopadhyay A, Machado FS, Belbin TJ, Campos de Carvalho A, Guan F, Albanese C, Jelicks LA, Lisanti MP, Silva JS, Spray DC, Weiss LM, Tanowitz HB, 2008. Alterations in myocardial gene expression associated with experimental *Trypanosoma cruzi* infection. *Genomics* 91: 423-432.
- Garg N, Popov VL, Papaconstantinou J, 2003. Profiling gene transcription reveals a deficiency of mitochondrial oxidative

- phosphorylation in *Trypanosoma cruzi*-infected murine hearts: implications in chagasic myocarditis development. *Biochim Biophys Acta* 1638: 106–120.
15. Rowin KS, Tanowitz HB, Wittner M, Nguyen HT, Nadal-Ginard B, 1983. Inhibition of muscle differentiation by *Trypanosoma cruzi*. *Proc Natl Acad Sci USA* 80: 6390–6394.
 16. Bertelli MS, Brener Z, 1980. Infection of tissue culture cells with bloodstream trypomastigotes of *Trypanosoma cruzi*. *J Parasitol* 66: 992–997.
 17. Fernandes O, Santos SS, Cupolillo E, Mendonça B, Derre R, Junqueira AC, Santos LC, Sturm NR, Naiff RD, Barret TV, Campbell DA, Coura JR, 2001. A mini-exon multiplex polymerase chain reaction to distinguish the major groups of *Trypanosoma cruzi* and *T. rangeli* in the Brazilian Amazon. *Trans R Soc Trop Med Hyg* 95: 97–99.
 18. Garzoni LR, Caldera A, Meirelles Mde N, de Castro SL, Docampo R, Meints GA, Oldfield E, Urbina JA, 2004. Selective *in vitro* effects of the farnesyl pyrophosphate synthase inhibitor riseridronate on *Trypanosoma cruzi*. *Int J Antimicrob Agents* 23: 273–285.
 19. Iacobas DA, Iacobas S, Li WE, Zoidl G, Dermietzel R, Spray DC, 2005. Genes controlling multiple functional pathways are transcriptionally regulated in connexin43 null mouse heart. *Physiol Genomics* 20: 211–223.
 20. Iacobas DA, Fan C, Iacobas S, Spray DC, Haddad GG, 2006. Transcriptomic changes in developing kidney exposed to chronic hypoxia. *Biochem Biophys Res Commun* 13: 329–338.
 21. Combs TP, Nagajyothi F, Mukherjee S, de Almeida CJ, Jelicks LA, Schubert W, Lin Y, Jayabalan DS, Zhao D, Braunstein VL, Landskroner-Eiger S, Cordero A, Factor SM, Weiss LM, Lisanti MP, Tanowitz HB, Scherer PE, 2005. The adipocyte as an important target cell for *Trypanosoma cruzi* infection. *J Biol Chem* 24: 24085–24094.
 22. Miles MA, Cedillos RA, Póvoa MM, de Souza AA, Prata A, Macedo V, 1981. Do radically dissimilar *Trypanosoma cruzi* strains (zymodemes) cause Venezuelan and Brazilian forms of Chagas' disease? *Lancet* 20: 1338–1340.
 23. Adesse D, Garzoni LR, Huang H, Tanowitz HB, de Nazareth Meirelles M, Spray DC, 2008. *Trypanosoma cruzi* induces changes in cardiac connexin43 expression. *Microbes Infect* 10: 21–28.
 24. de Melo TG, Meirelles Mde N, Pereira MC, 2008. *Trypanosoma cruzi* alters adherens junctions in cardiomyocytes. *Microbes Infect* 10: 1405–1410.
 25. Saffitz JE, Hames KY, Kanno S, 2007. Remodeling of gap junctions in ischemic and nonischemic forms of heart disease. *J Membr Biol* 218: 65–71.
 26. Celes MR, Torres-Dueñas D, Alves-Filho JC, Duarte DB, Cunha FQ, Rossi MA, 2007. Reduction of gap and adherens junction proteins and intercalated disc structural remodeling in the hearts of mice submitted to severe cecal ligation and puncture sepsis. *Crit Care Med* 35: 2176–2185.
 27. Spray DC, Tanowitz HB, 2007. Pathology of mechanical and gap junctional co-coupling at the intercalated disc: is sepsis a junctionopathy? *Crit Care Med* 35: 2231–2232.